Predictive biological activity of newly synthesized hydrazone compounds derived from indomethacin

Nora Amer Hussien, Hyffaa Y. Hussien, Shaymaa H. Abdulrahman*

Department of Chemistry, College of Science, University of Mosul, Mosul, Iraq
*Email: shaymaa.hashim@uomosul.edu.iq

Abstract

New derivatives of hydrazone have been successfully created, specifically 2-(1-(Aryl)-5-methoxy-2-methyl-1H-indol-3-yl)-N'-(2-chlorobenzylidene) acetohydrazide. The transformation of Indomethacin ester into hydrazide was achieved through a reaction with hydrazine hydrate in absolute ethanol, followed by the reaction of the resulting hydrazide with aromatic aldehydes. The structures of these newly synthesized hydrazones were validated through IR, 1HNMR, and 13CNMR analyses. Each compound's energies were optimized by utilizing density functional theory (DFT) for theoretical calculations. By employing a quantitative structure-activity relationship (QSAR) mathematical model, this optimization enables the prediction of the biological activity of the compounds. Therefore, this research centers on the synthesis and characterization of hydrazone derivatives of Indomethacin, emphasizing the use of QSAR modeling to connect biological activity and molecular structure. The study sheds light on the methods employed for compound synthesis and characterization, contributing valuable insights into the properties and potential applications of these innovative derivatives through the application of computational chemistry.
Keywords: Indomethacin, biological activity, QSAR, DFT.

Introduction

Indomethacin, recognized as a non-steroidal anti-inflammatory drug, exhibits noteworthy anti-inflammatory, antipyretic, and analgesic attributes. Its extensive application encompasses the alleviation of arthritis pain and fever (Gliszczyńska & Nowaczyk, 2021). On a different note, hydrazones display a myriad of utilities spanning antifungal (Popiołek, 2021), antiviral, anticancer

(Wahbeh & Milkowski, 2019), analgesic, anticonvulsant, antioxidant, and anti-inflammatory effects (Awantu et al., 2021).

A substantial body of evidence underscores the pharmacophoric nature of hydrazones, evident in their roles as α-glucosidase inhibitors and inhibitors of platelet aggregation on rabbit platelet-rich plasma (Fraga et al., 2000). Impressively, derivatives of hydrazones also find utility as corrosion inhibitors within acidic mediums (Lgaz, Chung, et al., 2020). Notably, recent work by Lgaz and colleagues involved the synthesis of a range of hydrazone derivatives through functionalization of the unbound carboxylic group in indomethacin (Lgaz, Salghi, et al., 2020). Noteworthy findings from their study reveal that these newly synthesized hydrazone derivatives originating from indomethacin offer enhanced resistance to corrosion for steel, particularly in solutions of 1.0 mol/L HCl and 15% HCl (Lgaz et al., 2019).

The QSAR constitutes a fundamental tool in comprehending the intricate interplay between a compound's biological activity and its molecular composition (Ahmad et al., 2017). The QSAR framework takes the form of a mathematical expression that establishes this connection, wherein the biological activity is treated as the reliant factor. At the same time, The independent variable in this context is the molecular structure of the compounds (Badawi et al., 2023; Irannejad et al., 2014; Jia et al., 2018; Pandey et al., 2020). The first step in developing a QSAR model is to transform the molecular structures of compounds into molecular descriptors, which are numerical representations. The formats of these descriptors are classified as follows: zero-dimensional (0D), one-dimensional (1D), two-dimensional (2D), and three-dimensional (3D) (Piir et al., 2018). During the QSAR modeling process, the selection of pertinent descriptors associated with biological activity gains paramount importance. An effective technique for this purpose is Interval Partial Least Squares (IPLS), which optimizes predictions by discerning a subset of variables from the dataset. IPLS entails the division of spectra into equidistant subintervals, followed by the construction of Partial Least Squares (PLS) models for each subinterval. Through an exhaustive search, the IPLS approach identifies the most pertinent variables or their combinations (Abdulrahman et al., 2022; Chen et al., 2019). The subsequent utilization of the PLS technique, a regression method, aims at unearthing correlations between molecular structure and properties. PLS accomplishes this by approximating and amplifying the correlation between the matrix of dependent variables (Y) and the matrix of molecular descriptors (X). In this context, the study's objective centers on formulating a dependable QSAR model for 1,3,4-oxadiazole derivatives. In conjunction with PLS, IPLS is utilized to select variables for this undertaking, which entails

regression analysis (Baviskar et al., 2020), as documented by Asadollahi et al. in 2014. After the availability of a mathematical model derived from a group of compounds derived from the same basic structure, this model is utilized to anticipate new compounds' biological activity that are not prepared or syntheses, and these values are calculated theoretically only. This method is considered one of the most important applications of the quantitative relationship between composition and effectiveness.

Methodology

Experimental methods

Melting points were ascertained using Gallen Kamp's melting point apparatus (from England) with open glass capillaries and are reported without corrections. KBr plates were utilized to acquire infrared spectra through a Pye Unicom SP 2000 instrument located at the College of Science, Mosul University. The 13C-NMR and 1H-NMR spectra were acquired on a Bruker 400 MHz spectrophotometer at the College of Science, Al-Basrah University, employing TMS as the internal standard in CDCl3 as the solvent.

The preparation of ethyl [1-(4-chlorobenzoyl)-2-methyl-5-methoxy-1H-indol-3-yl] acetate (Popiołek, 2021) **involves a standardized method outlined in General Procedure** (Wiklund & Bergman, 2006)**.**

To prepare the target compound, in 20 ml of absolute ethanol saturated with HCl gas, Indomethacin (Gliszczyńska & Nowaczyk, 2021), a solution of 0.01 mole (3.57 g) of Indomethacin was dissolved. The resulting mixture underwent reflux under a steam bath for 2 hours. Afterward, to room temperature, the flask contents were elegible to cool. After that, onto crushed ice, it was poured. Then, neutralized using ammonium solution. Through ether extraction, the resulting slurry was subjected. Filtration was performed, followed by reduced pressure evaporation of the organic layer that had been desiccated over anhydrous magnesium sulfate. The result of this procedure was a semi-solid product, which, when recrystallized from n-heptane, generated dazzling, white needle crystals with an 83% yield and a melting point of 90-92 °C. The synthesized compound was characterized by IR spectroscopy (KBr disk) with the following key peaks: 1717 cm-1 (C=O stretching, ester), 1660 cm-1 (C=O stretching, tertiary amide), 1522-1594 cm-1 (C-C stretching), 3073 cm-1 (aromatic C-H stretching), 2977 cm-1 (aliphatic C-H stretching), 1363 cm-1 (methyl group bending), and 761 cm-1 (C-Cl stretching).

Synthesis of [1-(4-chlorobenzoyl)-5-methoxy-2-methyl-1H-indol-3-yl] acetic acid hydrazide (Wahbeh & Milkowski, 2019)**:**

General Procedure (Selim et al., 2018)**:**

A solution was prepared by dissolving 3.85 grams (0.01 mole) of the ester (Popiołek, 2021) in 50 milliliters of absolute ethanol. To this solution, we added 0.72 milliliters (0.05 mole) of freshly distilled hydrazine hydrate, treated with sodium hydroxide. The resulting mixture underwent reflux for 48 hours. After cooling and collecting through filtration, the precipitate formed was separated. The collected material was subsequently recrystallized from dry benzene, resulting in the formation of white, luminous crystals of the hydrazide (Wahbeh & Milkowski, 2019) with a melting point of 158-160 °C, achieving an 81% yield. The infrared spectrum (IR) of the hydrazide (Wahbeh & Milkowski, 2019) in KBr pellets revealed characteristic peaks at ν cm-1: 1659 (C=O stretch, amide), 1487-1595 (C=O stretch, tertiary amide), 1613 (C=C stretch), 3307 (N-H stretch, amide), 3212, 3193 (NH2 stretch), 3011 (C-H stretch, aromatic), 2875 (C-H stretch, aliphatic), 1397 (CH3 bend), and 731 (C-Cl stretch).

Synthesis of N' -(arylidene)-2-(1-(4-chlorobenzoyl)-5-methoxy-2-methyl-1H-indol-3-yl) acetohydrazide (Awantu et al., 2021; Fraga et al., 2000; Lgaz et al., 2019; Lgaz, Chung, et al., 2020; Lgaz, Salghi, et al., 2020)**:**

General Procedure (Mashayekhi et al., 2013)

A solution of hydrazide (Wahbeh & Milkowski, 2019) (0.0005 moles, 0.2 g) and aldehydes (0.0005 moles) was prepared by dissolving them in 10 mL of ethanol. We placed the reaction mixture in a 25 mL flask equipped with a magnetic stirrer and subjected to reflux for 5 hours. Following the cooling and filtration of the mélange, the mixture was recrystallized from ethanol to obtain pure products (Awantu et al., 2021; Fraga et al., 2000; Lgaz et al., 2019; Lgaz, Chung, et al., 2020; Lgaz, Salghi, et al., 2020). Tables 1 and 2, respectively, list the physical properties and spectral information of compounds (Awantu et al., 2021; Fraga et al., 2000; Lgaz et al., 2019; Lgaz, Chung, et al., 2020; Lgaz, Salghi, et al., 2020).

Synthesis of N'-(benzo[d][1,3] dioxol-5-ylmethylene)-2-(1-(4-chlorobenzoyl)-5-methoxy-2-methyl-1H-indol-3-yl)acetohydrazide (Awantu et al., 2021)**.**

The compound synthesis Co, as detailed on pages 191-193, resulted in a white precipitate with a yield of 66%. The compound exhibits a distinct Rf value of 0.82. The infrared (IR) spectrum, recorded with KBr pellets, displayed characteristic peaks at ν cm-1: 1646 (indicating C=O stretching in amide and tertiary amide), 1626 (reflecting C=N stretching in aliphatic), 1589

(representing C=N and C=C stretching in aromatic), 3309 (N-H stretching in amide), 3007 (C-H stretching in aromatic), 2779 (C-H stretching in aliphatic), 1258 (C-O-C stretching asymmetry), and 1217 (C-O-C stretching symmetry). Additionally, the proton NMR (1H NMR) spectrum (400 MHz, CDCl3) revealed peaks at δ ppm: 2.10 (3H, s, CH3), 3.76 (2H, s, CH2), 4.05 (3H, s, OCH3), 5.91 (2H, s, CH2), 6.69-7.73 (11H, m, Ar-CH), 7.71 (1H, s, =CH), and 7.71 (1H, s, NH). The carbon-13 NMR (13C NMR) spectrum (100 MHz, CDCl3) exhibited signals at δ ppm: 169.02, 167.99, 155.90, 149.01, 148.25, 145.44, 137.16, 136.92, 132.43, 131.89, 131.23, 131.06, 129.17, 127.88, 121.59, 115.45, 111.90, 108.41, 108.20, 105.97, 102.01, 101.32, 55.72, 31.50, and 13.35.

Synthesis of 2-(1-(4-chlorobenzoyl)-5-methoxy-2-methyl-1H-indol-3-yl)-N'-(4-methoxybenzylidene) acetohydrazide (Fraga et al., 2000)

In the synthesis described on pages 143-145 of the referenced document, a white precipitate was obtained with a yield of 57%. The compound's characteristics were further analyzed, revealing a retention factor (Rf) of 0.59. Infrared spectroscopy (IR) using KBr pellets displayed distinctive peaks at ν cm-1: 1651 (indicative of C=O stretching in amide and tertiary amide), 1625 (associated with C=N stretching in aliphatic compounds), 1596 (attributed to C=N and C=C stretching in aromatic structures), 3265 (N-H stretching in amide), 1244 (asymmetric stretching of C-O-C), 1213 (symmetric stretching of C-O-C), 3033 (aromatic C-H stretching), and 2835 (aliphatic C-H stretching). The compound's 1H NMR spectrum (400 MHz, CDCl3) exhibited peaks at δ: 2.36 (3H, singlet, CH3), 3.84 (2H, singlet, CH2), 4.10 (6H, singlet, OCH3), 6.76-7.71 (11H, multiplet, Ar-CH), 7.97 (1H, singlet, NH). Additionally, the 13C NMR spectrum (100 MHz, CDCl3) displayed peaks at δ: 171.90, 167.68, 154.54, 138.23, 133.96, 131.01, 130.30, 129.05, 128.58, 128.30, 111.60, 111.28, 103.57, 99.92, 77.24, 55.94, 55.41, 30.61, and 11.74 ppm.

Synthesis of 2-(1-(4-chlorobenzoyl)-5-methoxy-2-methyl-1H-indol-3-yl) -N'-(2-chlorobenzylidene) acetohydrazide [N₆].

The compound synthesis Co was achieved with a satisfactory yield of 72%, as evidenced by a light-white precipitate (m.p 184-187°C). The compound was characterized by various analytical techniques. The thin-layer chromatography (TLC) analysis revealed an Rf value of 0.50. Infrared spectroscopy (IR) of KBr pellets displayed prominent peaks at ν cm⁻¹: 1648 (C=O stretching of amide and tertiary amide), 1597 (C=N stretching of aliphatic), 1568 (C=N and C=C stretching of aromatic), 3243 (N-H stretching of amide), 3034 (C-H stretching of aromatic), 2829 (C-H stretching of aliphatic), and 789 (C-Cl stretching). The 1H NMR spectrum (400 MHz, CDCl3) exhibited signals at δ ppm 2.39 (3H, s, CH3), 3.69 (2H, s, CH2), 4.14 (3H, s, OCH3), 6.74-8.28

(11H, m, Ar-CH), 8.79 (1H, s, =CH), and 9.07 (1H, s, NH). The 13C NMR spectrum (100 MHz, CDCl3) displayed peaks at δ ppm 144.25, 134.34, 131.37, 130.90, 129.06, 127.20, 127.08, 110.98, 110.91, 77.35, 77.24, 77.04, 76.72, 55.94, 55.74, and 31.60.

Synthesis of 2-(1-(4-chlorobenzoyl)-5-methoxy-2-methyl-1H-indol-3-yl)-N'-(pyridin-2-ylmethylene) acetohydrazide [N7].

A light-yellow precipitate was obtained with a yield of 37% (m.p. 189-191°C). The compound's purity and identity were confirmed by various analytical techniques. The thin-layer chromatography (TLC) revealed a single spot with an Rf value of 0.78. Infrared spectroscopy (IR) analysis (KBr pellets) displayed characteristic peaks at 1655 cm-1 (C=O stretch of amide and tertiary amide), 1630 cm-1 (C=N stretch of aliphatic), 1593 cm-1 (C=N, C=C stretch of aromatic), 3384 cm-1 (N-H stretch of amide), 3031 cm-1 (C-H stretch of aromatic), and 2831 cm-1 (C-H stretch of aliphatic). The 1H NMR spectrum (400 MHz, CDCl3) exhibited peaks at δ 2.42 (3H, s, CH3), 3.82 (2H, s, CH2), 4.12 (3H, s, OCH3), 6.71-8.17 (11H, m, Ar-CH), 8.62 (1H, s, =CH), and 8.83 (1H, s, NH). The 13C NMR spectrum (100 MHz, CDCl3) displayed characteristic peaks at δ 185.93, 168.47, 167.84, 164.94, 164.54, 162.68, 158.65, 147.55, 147.29, 144.02, 143.92, 142.95, 142.74, 142.24, 125.61, 125.31, 124.71, 118.41, 114.67, 114.25, 113.41, 91.01, 74.48, 69.69, and 45.41 ppm.

Synthesis of 2-(1-(4-chlorobenzoyl)-5-methoxy-2-methyl-1H-indol-3-yl)-N'-(pyridin-3-ylmethylene) acetohydrazide [N8].

A light-yellow precipitate was obtained with a yield of 37% according to the procedure outlined on pages 189-191 in the referenced source. The characterization of the synthesized compound was accomplished through various analytical techniques. The thin-layer chromatography (TLC) analysis revealed an Rf value of 0.78. The infrared (IR) spectrum of the compound, recorded using potassium bromide (KBr) pellets, exhibited characteristic peaks at 1655 cm-1 (C=O stretching of amide and tertiary amide), 1630 cm-1 (C=N stretching in aliphatic), 1593 cm-1 (C=N and C=C stretching in aromatic), 3384 cm-1 (N-H stretching of amide), 3031 cm-1 (C-H stretching in aromatic), and 2831 cm-1 (C-H stretching in aliphatic). Additionally, the 1H NMR spectrum (400 MHz, CDCl3) displayed signals at 2.42 ppm (3H, singlet, CH3), 3.82 ppm (2H, singlet, CH2), 4.12 ppm (3H, singlet, OCH3), 6.71-8.17 ppm (11H, multiplet, Ar-CH), 8.62 ppm (1H, singlet, =CH), and 8.83 ppm (1H, singlet, NH). The 13C NMR spectrum (100 MHz, CDCl3) revealed peaks at various chemical shifts, confirming the structural features of the compound.

Theoretical methods

In this study, we employed a systematic methodology to model the chemical structures of Indomethacin derivatives, adhering to a structured approach. Initially, ChemDraw Ultra version 11.0 was utilized to create two-dimensional representations, which were subsequently imported into Chem 3D-ChemBioOffice software (v. 16.0.0.82) for rigorous energy minimization at an ultra-level. In multiple steps, an optimization process is involved, starting with molecular mechanics calculations (MM2) followed by MMFF94 methods. The primary goal was to achieve a root mean square (RMS) gradient value below 0.1 kcal/mol, ensuring a negative heat of formation and positive frequency values.

Furthermore, semi-empirical calculations were integrated into the optimization process, utilizing the Parameterized Model 3 (PM3) and Austin Model 1 (AM1) methodologies. Until a minimal root mean square (RMS) gradient of 0.1 was attained, Density Functional Theory (DFT) computations utilizing the B3LYP level and a 6-311G basis set were indispensable (Atrushi et al., 2023). Gaussian 03w software was employed to predict descriptors, utilizing various techniques such as PM3, Hartree-Fock ab initio (HF), and DFT, chosen based on the specific descriptor type (Khalil & Abdulrahman, 2022). This comprehensive approach ensures a thorough analysis of the Indomethacin derivatives, combining computational and theoretical methods for a robust outcome.

Results And Discussions

Ethyl [1-(4-chlorobenzoyl)-5-methoxy-2-methyl-1H-indol-3-yl] acetate (Popiołek, 2021) was synthesized using the Buchman method. Indomethacin facilitated the synthesis with hydrochloric acid as a catalyst in an ethanolic solution. In absolute ethanol, the indomethacin ester (compound 2) has been condensed with hydrazine hydrate to produce α-(3-indomethacin acetyl hydrazine (Wahbeh & Milkowski, 2019). The hydrazide infrared spectrum (Wahbeh & Milkowski, 2019) exhibited alterations as the absorption band associated with the carbonyl ester ceased to exist at 1711 cm-1. The tertiary carbonyl amide and carbonyl hydrazide, respectively, were identified by the appearance of distinct absorption bands at 1654 cm-1 and 1631 cm-1, and a medium absorption band at 1631 cm-1 occurred in its place.

Hydrazone compounds (Awantu et al., 2021; Fraga et al., 2000; Lgaz et al., 2019; Lgaz, Chung, et al., 2020; Lgaz, Salghi, et al., 2020) were derived by condensing hydrazide (Wahbeh & Milkowski, 2019) with aldehydes. The formation mechanism of hydrazones likely involves an addition-elimination reaction (Ehrenson, 1964). The IR spectra of compounds (Awantu et al., 2021; Fraga

et al., 2000; Lgaz et al., 2019; Lgaz, Chung, et al., 2020; Lgaz, Salghi, et al., 2020) (see Table 1) displayed absorption bands at 3205-3384 cm-1 for N-H, 1646-1661 cm-1 for the C=O group, and 1589-1597 cm-1 for the C=N stretching absorption.
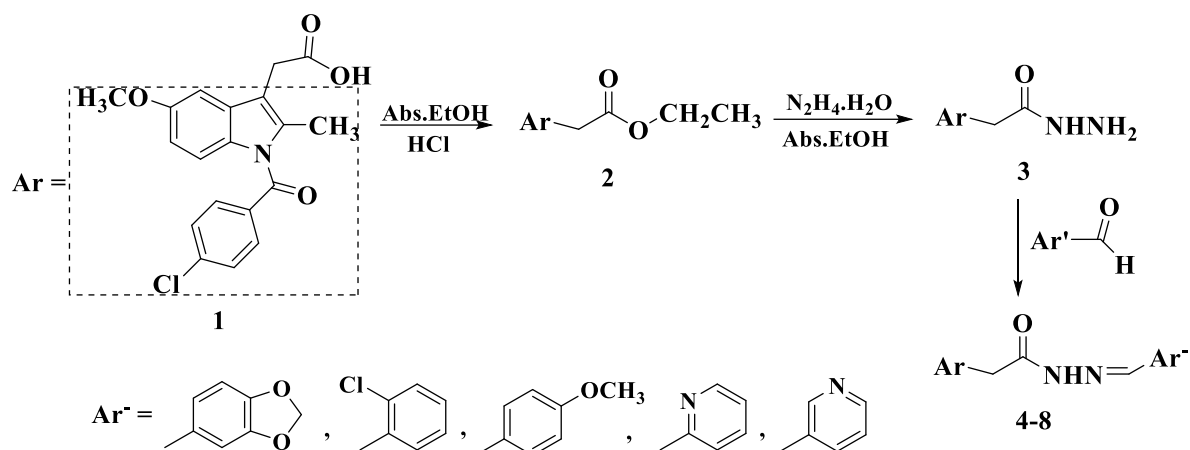
Scheme 1. Some hydrazone compounds synthesis.

Quantum Chemical Calculations

Approximations for the exchange-correlation energy function were computed to evaluate the reliability of eight compounds. Figure 1 presents visual representations of the three-dimensional structures of the Lowest Unoccupied Molecular Orbital (LUMO) and Highest Occupied Molecular Orbital (HOMO).
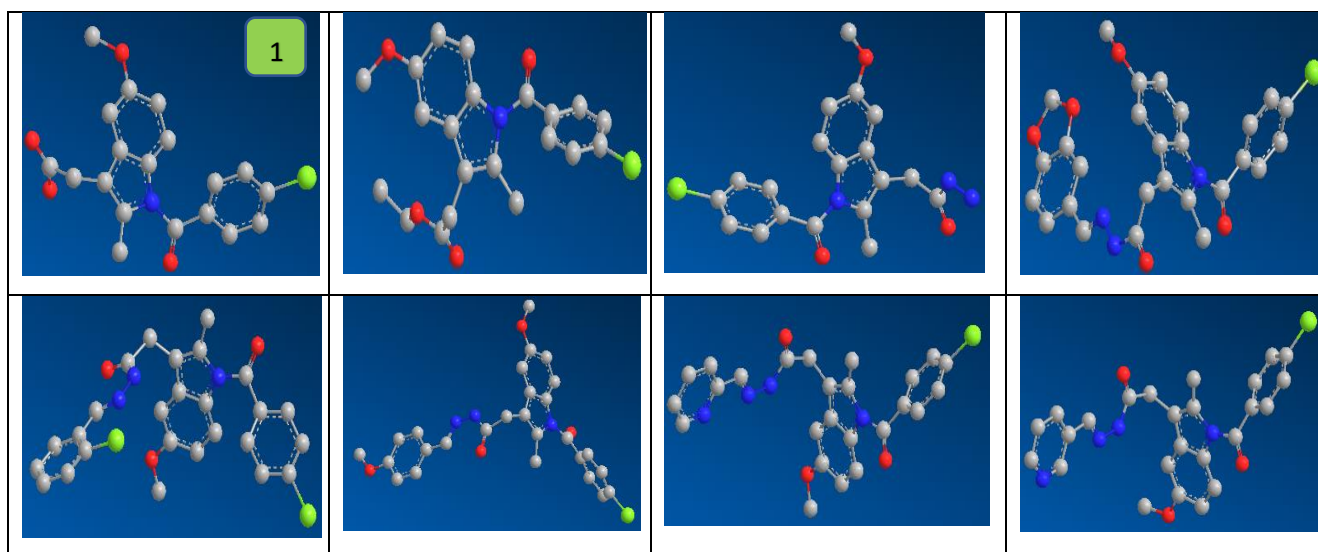
Figure 1. 3D molecular structures after minimum energy of compounds 1-8

Computational programs are very important in reducing time and effort in addition to the cost of studying and preparing chemical compounds. A series of theoretical calculations were made for the prepared compounds, the most important of which is calculating the energy values (HOMO & LUMO), which represent the stability of the compounds, from which several descriptors were calculated for the compounds under study, which are shown in Table 1.

Table 1. LUMO and HOMO energies calculation, as well as some descriptors of compounds 1-8.

No.	HOMO (eV)	LUMO (eV)	GAP	Ion.Pot. (I)	E.Aff. (A)	Chem.Pot (μ)	Hard. (η)	Soft. (S)	E.G (x)	Electroph. (ω)
1	-0.22155	-0.06856	0.15299	0.22155	0.06856	0.145055	0.076495	13.07275	-0.14506	0.137532
2	-0.28994	0.08973	0.37967	0.28994	-0.08973	0.100105	0.189835	5.267733	-0.10011	0.026394
3	-0.30059	0.08449	0.38508	0.30059	-0.08449	0.10805	0.19254	5.193726	-0.10805	0.030318
4	-0.29245	0.08758	0.38003	0.29245	-0.08758	0.102435	0.190015	5.262742	-0.10244	0.027611
5	-0.29997	0.0883	0.38827	0.29997	-0.0883	0.105835	0.194135	5.151055	-0.10584	0.028849
6	-0.29008	0.08281	0.37289	0.29008	-0.08281	0.103635	0.186445	5.363512	-0.10364	0.028803
7	-0.30037	0.0794	0.37977	0.30037	-0.0794	0.110485	0.189885	5.266345	-0.11049	0.032143
8	-0.2975	0.07954	0.37704	0.2975	-0.07954	0.10898	0.18852	5.304477	-0.10898	0.0315

A mathematical model was used derived from a previous study of indomethacin derivatives prepared in the laboratory and diagnosed by multiple and different diagnostic methods, and then it was studied computationally and a mathematical model was designed to predict the biological activity, which is equation below (Hanna, 2012).

Anti-inflammatory (% inhibition) = - 5.43095 - 1.54154 (No.O2) - 10.18241 log P + 464.65895 CPP + 2.64391 MR + 9.17934 D

Where this model was applied to the compounds prepared in our study, which are also derivatives of indomethacin, after making all the calculations required to apply the model and calculating the biological activity value theoretically and as shown in Table 2.

Table 2. The predicted activity values and molecular descriptor values of the anti-inflammatory activities of the compounds

NO.com	M.Wt. (g/mol)	TPSA (A^2)	No. of Oxygen atom	C log P	CPP	Mol.Ref.	Dipol.mome. (Debye)	Predicted activity (% inhibition)
1	357.790	66.84	4	3.580	0.001595	9.505	3.771	12.4427
2	385.844	55.84	4	4.291	0.001499	10.432	3.973	9.45737
3	371.821	84.66	3	2.793	0.001491	10.089	4.650	31.5563
4	503.939	89.46	5	5.243	0.001562	13.783	5.846	24.3042
5	494.372	71.00	3	6.021	0.001557	13.682	2.191	-14.351
6	489.956	80.23	4	5.337	0.001568	13.808	3.546	3.84114
7	460.918	83.36	3	4.550	0.001553	12.981	4.452	19.5223
8	460.918	83.36	3	4.126	0.001559	12.980	4.402	23.3768

We note that most of the indomethacin substitute compounds showed biological activity in varying proportions. The fifth compound showed a negative value for the biological activity percentages, and the reason for this was due to several factors that gathered and showed negative values, which can be interpreted as that this compound has no biological activity compared to other compounds of the same prepared group (Farrag, 2016).

Conclusion

In this investigation, derivatives of indomethacin were synthesized using approved chemical methods within the same laboratory conditions. The synthesis of these compounds was verified through various diagnostic measurements, including nuclear magnetic resonance and infrared radiation, along with fundamental physical measurements like melting points. Exploring the relationship between molecular structures and bio-activity, computational chemistry emerged as a pivotal tool. Predicting the biological activity of newly synthesised compounds via in silico methods has become increasingly prevalent in recent decades. To achieve this, a predetermined mathematical model specific to indomethacin-derived compounds was employed, predicting the biological activity values for the compounds under scrutiny. The diverse activities observed in the prepared compounds were attributed to variations in chemical composition and the distinctive compensating and active groups present in each compound. Remarkably, Compound No. 3 exhibited the highest biological activity, while Compound No. 5 displayed the lowest, with a negative value. This discrepancy resulted from the low descriptors values coupled with a positive

coefficient for Compound No. 5, contrasting with higher coefficients for the remaining compounds.

Acknowledgments

References

Abdulrahman, S. H., Al-khayat, R. Z., Alhamdany, A. Y., & Ali, W. K. (2022). QSAR of antioxidant activity of some novel sulfonamide derivatives. Egyptian Journal of Chemistry, 65(8), 489–497.

Ahmad, M. M., Alwi, S. R. W., Jamaludin, R., Chua, L. S., & Mustaffa, A. A. (2017). Quantitative structure-activity relationship model for antioxidant activity of flavonoid compounds in traditional chinese herbs. Chemical Engineering Transactions, 56, 1039–1044.

Atrushi, K. S., Ameen, D. M., Abdulrahman, S. H., & Abachi, F. T. (2023). Density Functional Theory, ADME, and Molecular Docking of Some Anthranilic Acid Derivatives as Cyclooxygenase Inhibitors.

Awantu, A. F., Ayimele, G. A., Bankeu, J. J. K., Nantia, E. A., Fokou, P. V. T., Boyom, F. F., Nfor, E. N., Lenta, B. N., & Ngouela, S. A. (2021). Synthesis, Molecular Structure, Anti-Plasmodial, Antimicrobial and Anti-Oxidant Screening of (E)-1-(Phthalazin-1-yl)-1-[(Pyridin-2-yl) Ethylidene] Hydralazine and 1-[2-(1-(pyridine-3-yl) ethylidene) hydrazinyl] phthalazine. International Journal of Organic Chemistry, 11(03), 91–105.

Badawi, W. A., Rashed, M., Nocentini, A., Bonardi, A., Abd-Alhaseeb, M. M., Al-Rashood, S. T., Veerakanellore, G. B., Majrashi, T. A., Elkaeed, E. B., & Elgendy, B. (2023). Identification of new 4-(6-oxopyridazin-1-yl) benzenesulfonamides as multi-target anti-inflammatory agents targeting carbonic anhydrase, COX-2 and 5-LOX enzymes: synthesis, biological evaluations and modelling insights. Journal of Enzyme Inhibition and Medicinal Chemistry, 38(1), 2201407.

Baviskar, B. A., Deore, S. L., & Jadhav, A. I. (2020). 2D and 3D QSAR studies of saponin analogues as antifungal agents against Candida albicans. Journal of Young Pharmacists, 12(1), 48.

Chen, C., Nie, Y., Xu, G., Yang, X., Fang, H., & Hou, X. (2019). Design, synthesis and preliminary bioactivity studies of indomethacin derivatives as Bcl-2/Mcl-1 dual inhibitors. Bioorganic & Medicinal Chemistry, 27(13), 2771–2783.

Ehrenson, S. (1964). Theoretical Interpretations of the Hammett and Derivative Structure-Reactivity Relationships. Progress in Physical Organic Chemistry, 195–251.

Farrag, A. M. (2016). Synthesis and biological evaluation of novel indomethacin derivatives as potential anti-colon cancer agents. Archiv Der Pharmazie, 349(12), 904–914.

Fraga, A. G. M., Rodrigues, C. R., de Miranda, A. L. P., Barreiro, E. J., & Fraga, C. A. M. (2000). Synthesis and pharmacological evaluation of novel heterotricyclic acylhydrazone derivatives, designed as PAF antagonists. European Journal of Pharmaceutical Sciences, 11(4), 285–290.

Gliszczyńska, A., & Nowaczyk, M. (2021). Lipid formulations and bioconjugation strategies for indomethacin therapeutic advances. Molecules, 26(6), 1576.

Hanna, M. M. (2012). New pyrimido [5, 4-e] pyrrolo [1, 2-c] pyrimidines: Synthesis, 2D-QSAR, anti-inflammatory, analgesic and ulcerogenicity studies. European Journal of Medicinal Chemistry, 55, 12–22.

Irannejad, H., Kebriaieezadeh, A., Zarghi, A., Montazer-Sadegh, F., Shafiee, A., Assadieskandar, A., & Amini, M. (2014). Synthesis, docking simulation, biological evaluations and 3D-QSAR study of 5-Aryl-6-(4-methylsulfonyl)-3-(metylthio)-1, 2, 4-triazine as selective cyclooxygenase-2 inhibitors. Bioorganic & Medicinal Chemistry, 22(2), 865–873.

Jia, Q., Zhao, Y., Yan, F., & Wang, Q. (2018). QSAR model for predicting the toxicity of organic compounds to fathead minnow. Environmental Science and Pollution Research, 25, 35420–35428.

Khalil, R. A., & Abdulrahman, S. H. (2022). Newly developed statistically intensive QSAR models for biological activity of isatin derivatives. Studia Universitatis Babes-Bolyai, Chemia, 67(1), 139–152.

Lgaz, H., Chung, I.-M., Albayati, M. R., Chaouiki, A., Salghi, R., & Mohamed, S. K. (2020). Improved corrosion resistance of mild steel in acidic solution by hydrazone derivatives: An experimental and computational study. Arabian Journal of Chemistry, 13(1), 2934–2954.

Lgaz, H., Salghi, R., Masroor, S., Kim, S.-H., Kwon, C., Kim, S. Y., Yang, Y.-J., & Chung, I.-M. (2020). Assessing corrosion inhibition characteristics of hydrazone derivatives on mild steel in HCl: Insights from electronic-scale DFT and atomic-scale molecular dynamics. Journal of Molecular Liquids, 308, 112998.

Lgaz, H., Zehra, S., Albayati, M. R., Toumiat, K., El Aoufir, Y., Chaouiki, A., Salghi, R., Ali, I. H., Khan, M. I., & Chung, I.-M. (2019). Corrosion inhibition of mild steel in 1.0 M HCl by two hydrazone derivatives. International Journal of Electrochemical Science, 14(7), 6667–6681.

Mashayekhi, V., Tehrani, K. H. M. E., Amidi, S., & Kobarfard, F. (2013). Synthesis of novel indole hydrazone derivatives and evaluation of their antiplatelet aggregation activity. Chemical and Pharmaceutical Bulletin, 61(2), 144–150.

Pandey, S. K., Ojha, P. K., & Roy, K. (2020). Exploring QSAR models for assessment of acute fish toxicity of environmental transformation products of pesticides (ETPPs). Chemosphere, 252, 126508.

Piir, G., Kahn, I., García-Sosa, A. T., Sild, S., Ahte, P., & Maran, U. (2018). Best practices for QSAR model reporting: physical and chemical properties, ecotoxicity, environmental fate, human health, and toxicokinetics endpoints. Environmental Health Perspectives, 126(12), 126001.

Popiołek, Ł. (2021). Updated information on antimicrobial activity of hydrazide–hydrazones. International Journal of Molecular Sciences, 22(17), 9389.

Selim, Y. A., Abd El-Azim, M. H. M., & El-Farargy, A. F. (2018). Synthesis and Anti-inflammatory Activity of Some New 1, 2, 3-Benzotriazine Derivatives Using 2-(4-Oxo-6-phenylbenzo [d][1, 2, 3] triazin-3 (4H)-yl) acetohydrazide as a Starting Material. Journal of Heterocyclic Chemistry, 55(7), 1756–1764.

Wahbeh, J., & Milkowski, S. (2019). The use of hydrazones for biomedical applications. SLAS TECHNOLOGY: Translating Life Sciences Innovation, 24(2), 161–168.

Wiklund, P., & Bergman, J. (2006). The chemistry of anthranilic acid. Current Organic Synthesis, 3(3), 379–402.